Application of MRF-based Stochastic Joint Inversion of Transient Hydraulic Head and Electrical Resistivity Measurements to Identify 2D Fracture Zone Connectivity

Guoqun Zhang & Erasmus K. Oware, *Department of Geology, University at Buffalo, SUNY*

University at Buffalo
The State University of New York

Contact Information:
guoqunzh@buffalo.edu
erasmuso@buffalo.edu

NS41B-1906

NS41B-1906

Abstract

Accurate quantification of the geometric and hydraulic (K) properties of fracture zones (FZs) and their connectivity is crucial to the management of groundwater resources. The widely used equivalent porous medium approach is inadequate to predict fracture transport processes due to the averaging of the sharp K contrast between the matrix and the FZs. Geophysics provide a viable opportunity for high resolution imaging of spatially continuous properties of fractured systems.

Traditional geophysical imaging strategies, however, produce smoothed-out fracture features. A recently developed Markov random field (MRF)-based stochastic imaging produces geologically realistic sharp lithologic contrast. The strategy infers site-specific statistics from hydrogeophysical measurements and applies the calibrated statistics for reconstruction.

We present here the first field-scale application of the algorithm. We demonstrate the strategy with field-scale pumping tests and 2D cross-borehole electrical resistivity experiments. We show, from joint inversion of the hydrogeophysical measurements, that the strategy is able to accurately delineate non-smooth FZs and their connectivity with fairly good correlations with FZs identified from optical borehole images from the two wells.

Introduction

Application of hydrogeophysical inverse modeling is becoming increasingly indispensable in groundwater resource management. Fig. 1 presents a flow chart for the motivation for this research.

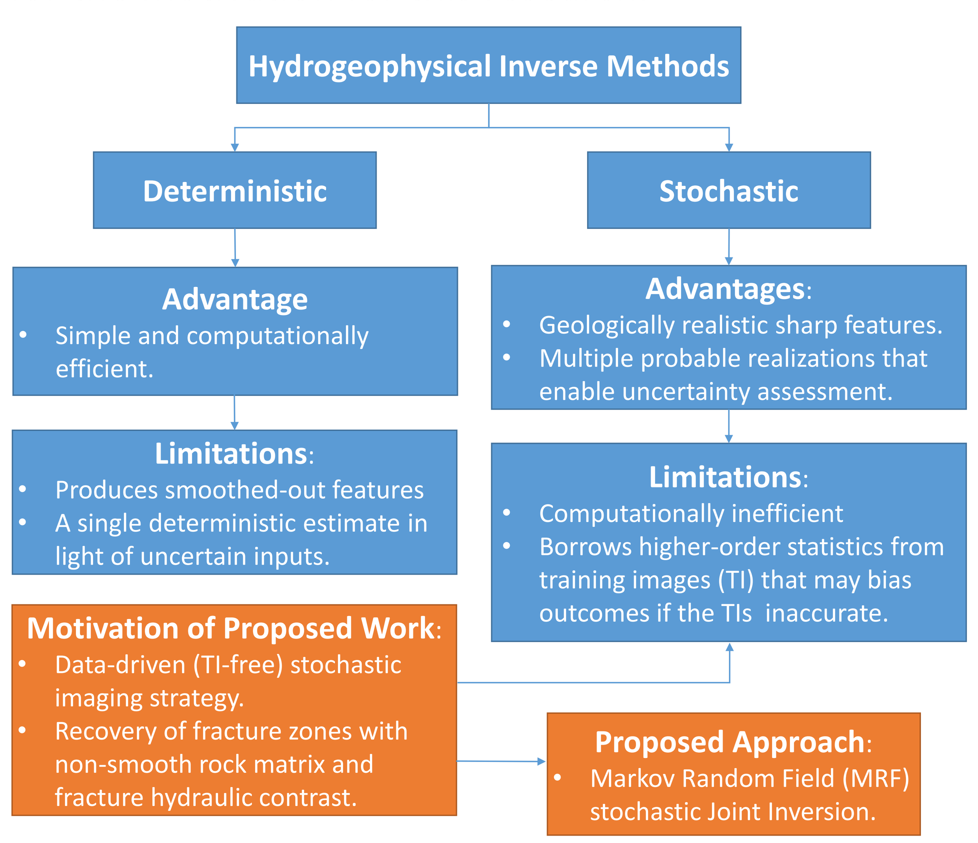

Figure 1: Motivation for the proposed work.

Modeling Methodology

MRF Basics

Neighborhood System and Cliques

Markov Random Field (MRF) modeling is based on cliques in a neighborhood system (Fig. 2).

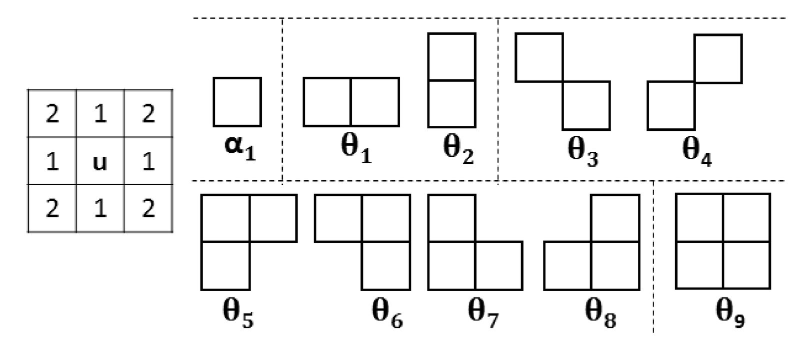

Figure 2: A 2nd order neighborhood system and all possible clique configurations. The α's and θ's represent the parameters of a Gibbs distribution (GD), which captures **spatial statistics, like size, orientation, and clustering.**

Gibbs Energy Estimation

Potential (Gibbs) energy (Eq. 1) serves as a guide to searching for the minimal solution. The smaller the Gibbs energy the higher the likelihood and vice versa [*Derin and Elliot*, 1987].

$$E = \sum_{u=1}^{n} \boldsymbol{\phi}^T(k(u), \mathbf{k}(\aleph_u))\theta \qquad (1)$$

where $k(u)$ is the central pixel value, $\mathbf{k}(\aleph_u)$ are the neighboring pixel values, $\phi(\cdot)$ is an indicator function that assess how the pixels interact in a clique (Eq. 2); and the vector θ contains the GD parameters (spatial statistics) of the various clique configurations (Fig. 2).

$$\phi(k(u), \mathbf{k}(\aleph_u)) = \begin{cases} -1 & \text{if all } \mathbf{k}(\aleph_u) \text{ equals to } k(u) \\ -0.5 & \text{if at least one } \mathbf{k}(\aleph_u) \text{ equals to } k(u) \\ 1 & \text{if none of } \mathbf{k}(\aleph_u) \text{ equals to } k(u) \end{cases} \qquad (2)$$

Modeling Algorithm

Fig. 3 shows the flow chart of the estimation algorithm, which involves a two-step simulation process.

Representative Hydraulic conductivity (K) and Resistivity Values for Rock Matrix and Fracture Facies

- K distribution for fractures: log-normal distribution with mean 4e-4 m/s [estimated from slug tests] and variance ln(K)=0.5.
- K distribution for rock matrix (shale and dolomite): log normal distribution with mean 1e-7 m/s and variance ln(K)=0.5.
- Expected resistivity range for fractures (fracture in-fill is weathered gypsum or shale): 5 – 100 Ohm.m
- Expected resistivity range for rock matrix (shale and dolomite): 5 – 100,000 Ohm.m

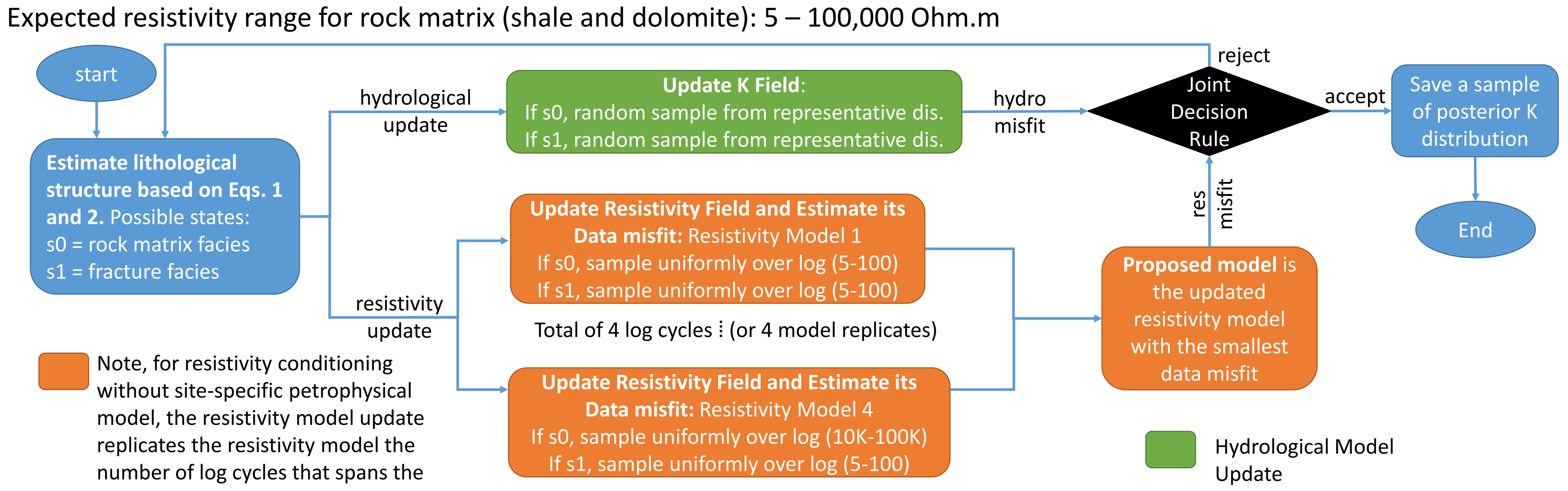

Figure 3: Flow chart for modeling algorithm.

Data-Driven GD Parameter Estimation

- Prior GD parameters (ones) are employed to initiate the algorithm in Fig. 3. The GD parameters are resimulated in an iterative manner conditional on the hydrological and geophysical measurements [*see Oware* (2016) for details].

Field Experiments

The field experiments were performed at the University at Buffalo Environmental Geophysics Imaging Site (UBEGIS).

Pumping Test Experiments

- Two open boreholes with pumping at different rates in one well at a time with drawdown monitoring in both wells (Figs. 4)
- Well 1 pumping: 10 and 20 gal/min, for Exps. 1 and 2, respectively.
- Well 2 pumping: 10, 20, and 30 gal/min Exps. 3, 4, 5, respectively.
- Well 2 step pumping at 40 to 30 gal/min for Exp. 6.

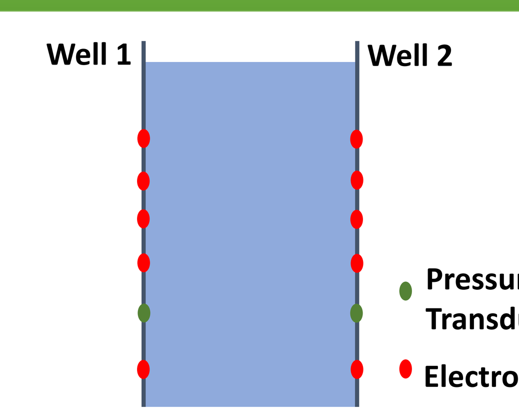

Figure 4: Pumping test and Cross-borehole electrical resistivity setup.

Pumping Tests Drawdown Data

The drawdown data from all the six experiments (Fig. 5) indicate higher drawdowns in well 1 (w1) compared to drawdowns in w2, suggesting possible higher fracture intensity in w2 in contrast to fracture intensity in w1.

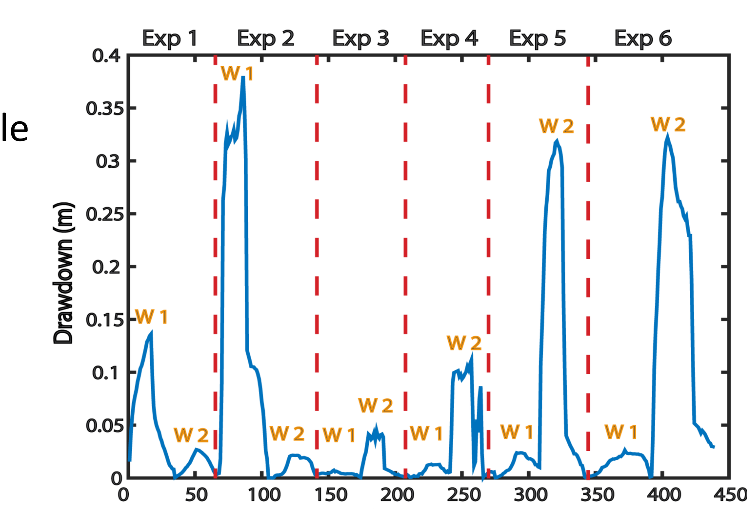

Figure 5: Drawdown from pumping tests.

Cross-Borehole Electrical Resistivity Survey

- 32 electrodes in each well with 0.5 m electrode spacing.
- Circulating dipole-dipole with full reciprocal measurements to acquire 6682 measurements.

HydroGeoSphere [*Brunner and Simmons*, 2012] and FW_2.5D [*Pidlisecky and Knight*, 2008] were used for the pumping test and resistivity forward simulations, respectively.

Results & Discussions

Joint Inversion with Data Unconditioned GD Parameters

- Fig. 6 shows inversion results based on only the prior information captured in Eq. 2, meaning all GD parameters (Eq. 1) were set to either 1 or -1.
- The uncertainty plot (Fig. 6) suggests that while the identified fracture zone (FZ) in the top right corner and features from about 9.5 m to 12 m depths seem fairly resolved, the FZ and connectivity were mostly poorly estimated.
- The generally high uncertainty in the estimation (Fig. 6) implies that only the prior information in Eq. 2 is inadequate for the reconstruction.

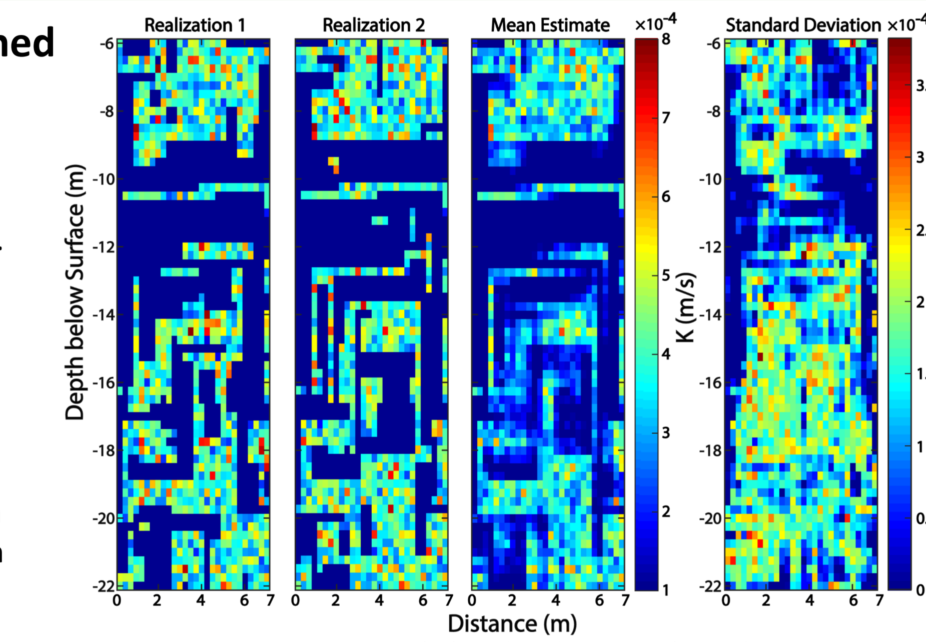

Figure 6: Joint inversion results based on data-unconditioned GD parameters.

Joint Inversion with Data Conditioned GD Parameters

Data-Driven GD Parameter (Statistics) Estimation

- The posterior mean (Fig. 7) for the estimated GD parameters are 1.2, 0.9, -1.1, -1.1, 1.1, 1.1, -0.9, -1.0, and 1.0, representing θ_1, θ_2, θ_3, θ_4, θ_5, θ_6, θ_7, θ_8, and θ_9 (see Fig. 2 for their matching cliques), respectively.
- While most of the posterior means differed by about 0.1 from the prior values of 1, the horizontal GD parameter (θ_1) witnessed the biggest increase, suggesting the dominance of horizontal features.

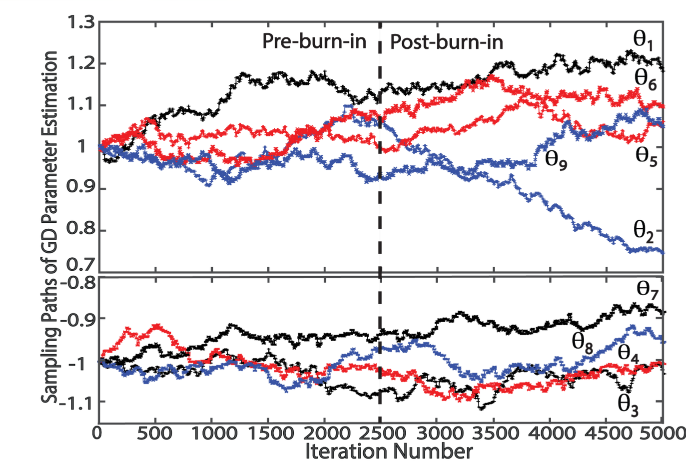

Figure 7: Sampling paths of the GD parameter estimation.

Reconstruction based on Data-Calibrated GD Parameter

- The data-calibrated statistics significantly improved the identification of the FZ and connectivity (Fig. 8) compared to those obtained in the case of data unconditioned GD parameters (Fig. 6).
- The standard deviation plot (Fig. 8) indicates that while two main FZs around 6-8 m and 20-22 m depths were identified, their edges were poorly resolved.
- There seems to be low FZ intensity from about 8-18 m with two main identified fractures in the interval connecting the two wells.
- There appears to be a higher FZ intensity in well 2 compared to those in well 1, which corroborates the low drawdowns observed in well 2 in contrast to those associated with well 1 (Fig. 5).

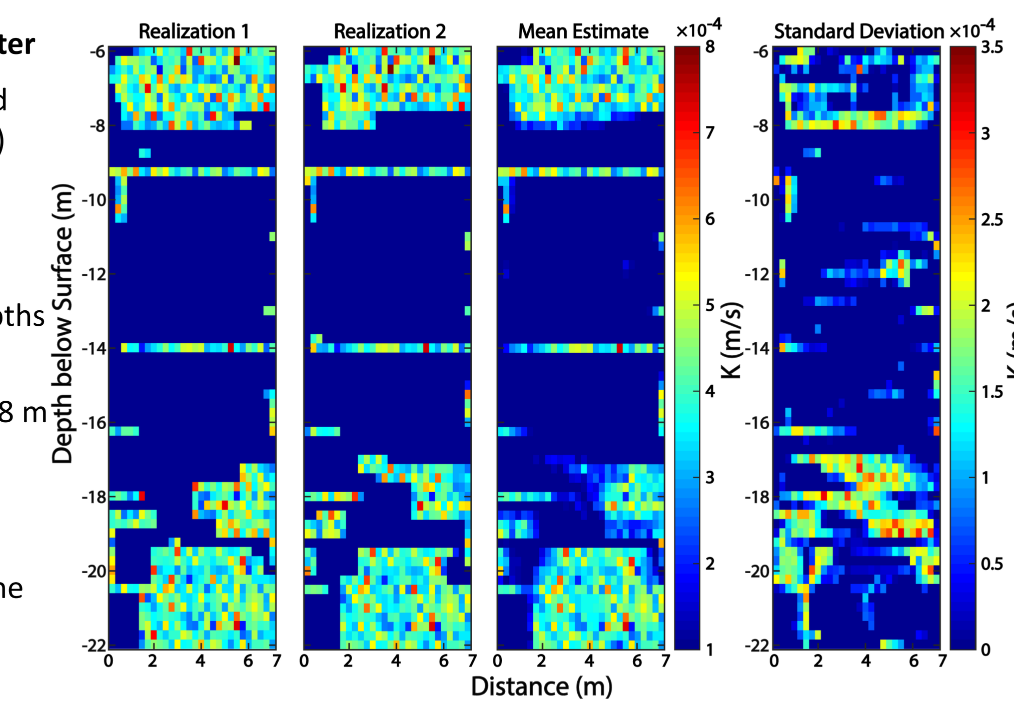

Figure 8: Joint inversion results based on data-conditioned GD parameters.

Model Validation with Optical Borehole Images (OBIs)

- A correlation of the estimated and OBI identified FZs (Fig. 9) reveal that while not all the OBI identified FZs were estimated, estimated FZs that are also identified in the OBIs seem well resolved (Figs. 8 and 9).

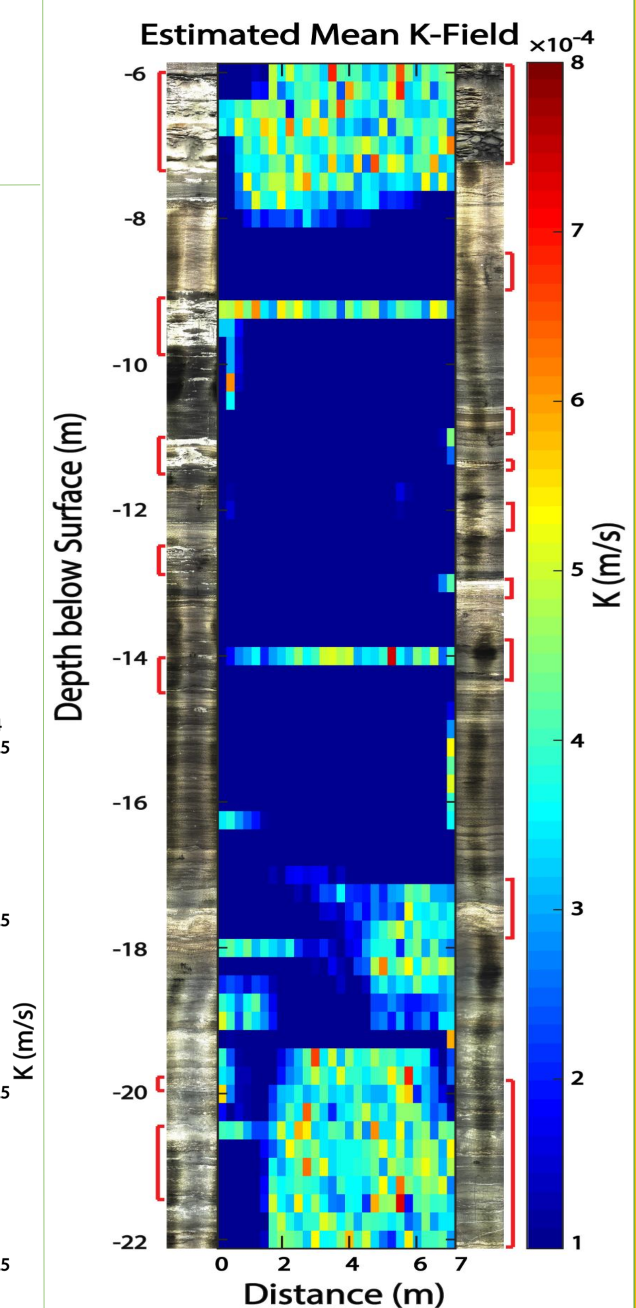

Figure 9: Estimated K field vs. OBI. OBI identified fracture zones are marked with red brackets.

Conclusion

- The preliminary results of the first field application of the MRF-based stochastic joint inversion to identify FZ and connectivity seem promising, with estimation of geologically realistic sharp matrix and FZ boundaries.
- While the data unconditioned GD parameters poorly resolved FZ and connectivity, the performance of the data-calibrated GD parameters improved significantly with higher certainty associated with estimated FZs that are also identified in the OBIs.
- There is mis- or non-identification of some of the FZs identified in the OBIs, which is plausibly attributable to the inability of the 2D FZ model to fully explain the actual 3D pumping test response.

Future Research Direction

- Development of a 3D version of the algorithm.
- Development of a site-specific petrophysical model that accounts for surface conduction (high shale) to convert the updated K model directly into a resistivity model for the joint inversion.

References

- Oware, E. K. (2016), Estimation of hydraulic conductivities using higher-order MRF-based stochastic joint inversion of hydrogeophysical measurements, *The Leading Edge.*, 35(9), 776-785.
- Derin, H., and H. Elliott (1987), Modeling and segmentation of noisy and texture images using Gibbs random fields, *IEEE Trans. Pattern Analysis and Machine Intelligence.*, 9, 39-55.
- Hammersley, J. M. and P. Clifford (1971), Markov field on finite graphs and lattices, unpublished.
- Brunner and Simmons (2012), HydroGeoSphere: a fully integrated, physically based hydrological model, *Groundwater.*, 50(2), 170-176, doi: 10.1111/j.1745-6584.2011.00882.x.
- Pidlisecky, A., and R.J. Knight (2008), FW2_5D: A MATLAB 2.5-D electrical resistivity modeling code, *Computers & Geosciences.*, 34(12), 1645-1654.